RELAXATION OF CONDUCTION ELECTRON SPINS AT COLLISIONS WITH GRAPHITE INTERCALATION FRONT

A.M. Ziatdinov and A.N. Krivoshei
Institute of Chemistry, Far Eastern Branch of the Russian Academy of Sciences
159, Prosp. 100-letiya, 690022 Vladivostok, Russia

Introduction

In spite of numerous publications devoted to studies of various aspects of graphite intercalation compounds (GICs) structure and properties [1-3], many aspects of mechanism of "guest" molecule intercalation into graphite have not received sufficient attention. The Conduction ESR (CESR) technique is one of the most powerful methods for studying the graphite intercalation process, because shapes and intensities of the CESR signal both from non-intercalated and intercalated regions of graphite plate vary strongly during the intercalation. However, because of the difficulty of such experiments only a few CESR studies of graphite intercalation process have been undertaken [4-9]. But even in these cases, because of presence of the skin effect, the interpretation of changes in the graphite CESR signal during the intercalation process is difficult.

This paper is devoted to the results of an *in situ* CESR study of HNO_3 molecule intercalation into narrow HOPG slabs (with width being comparable with the skin-depth δ_c governed by the graphite ***c***-axis conductivity σ_c). The analysis of these results uniquely points to the presence of the strong interface spin relaxation effects in samples investigated. The results of a theoretical analysis of the reasons for an increase of graphite and GIC CESR signal linewidth during intercalation are also presented.

Experimental

CESR measurements were carried out at room temperature using an X-band E-line spectrometer in a rectangular cavity with TE_{102} mode. The constant magnetic field ($\boldsymbol{H}_0$) modulation frequency and amplitude were 2.5 kHz and 0.1 mT, respectively.

All experiments were carried out on samples in the shape of rectangular parallelepipeds with the dimensions: width (l)×height (h)×thickness (d), where $h \times l$ is the area of the basal plane. At the experiments, the basal $l \times h$ and lateral $d \times h$ sides were parallel and the ***c***-axis was perpendicular to the magnetic component ($\boldsymbol{H}_{rf}$), of the microwave field (Fig. 1). Note, that in the rectangular resonator, the structure of electromagnetic field of TE_{102} mode has such a form that, at a conventional setting of the resonator, $\boldsymbol{H}_0$ is parallel to the electrical component ($\boldsymbol{E}_{rf}$) of microwave field (Fig. 1).

The CESR study of graphite intercalation by nitric acid was carried out on HOPG plates with dimensions: 0.4×0.04×0.02 cm^3 and 0.4×0.045×0.03 cm^3. The HOPG samples were held in quartz tube connected via a valve to the reservoir with intercalate (liquid HNO_3 with density $\rho \cong 1.565$ g/cm^3). Nitric acid vapours penetrated into

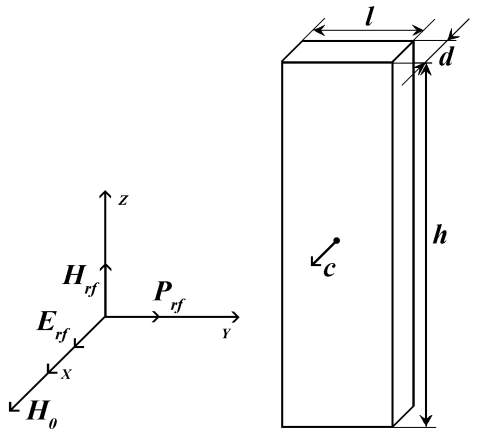

Figure 1. The orientation of the HOPG slab with respect to the external magnetic field $\boldsymbol{H}_0$ and the cavity axis (X, Y and Z). $\boldsymbol{H}_{rf}$, $\boldsymbol{E}_{rf}$ and $\boldsymbol{P}_{rf}$ are the magnetic and electric components of the radio-frequency field, and the Pointing vector in an unloaded rectangular cavity, respectively.

the knee of reactor with the graphite sample through the hole with the size ≈8×10^{-3} cm^2 in the fluoroplastic diaphragm. Prior to the experiment, the system was evacuated to eliminate air and water. During the measurements, $\boldsymbol{H}_0$ was applied along the graphite ***c***-axis.

According to data of the four-probe method, at 300 K the ***c***-axis conductivity (σ_c) of HOPG plate used is equal to (7.7±0.8) S/cm. In the X-band experiment the value of the skin depth δ_c~0.02 cm corresponds to this conductivity, i. e. in experiments of graphite intercalation by nitric acid the whole volume of the HOPG plate investigated was available for the CESR studies.

Results

For HOPG plates studied the CESR spectrum consists of a single asymmetric line determined by Dyson mechanism [10] and with the principal values of g – factor equal to: g_c=2.0474±0.0002 ($\boldsymbol{H}_0 \| \boldsymbol{c}$) and g_a=2.0029±0.0002 ($\boldsymbol{H}_0 \perp \boldsymbol{c}$).

After outflow of certain time (so-called "induction" time depending on sample size and experimental conditions) after the injection of HNO_3 gas into the knee of the reactor with the HOPG plate, the CESR signal of graphite begins to transform and decrease in intensity until it fully disappears (Fig. 3). Simultaneously a new signal with g_c*=2.0019±0.0002, and g_a*=2.0030±0.0002 appears in the spectrum (Fig. 3), where g_i*(i=a, c) value is determined by the H_0 value at the point of intersection of the first derivative of CESR absorption line and the base line.

The linewidth (the intensity), ΔH ($I=(A+B)\times\Delta H^2$), of the graphite CESR signal increases (decreases) vs. exposure time, τ, monotonously (Fig. 2 and 4). In an initial HOPG sample, which was used in experiment on intercalation, the CESR lineshape is 'normal' in the sense that the maximum peak height occurs at the lower magnetic fields. At the beginning of reaction the A/B ratio of graphite signal increases, but it is still 'normal' reaching a maximum value of $A/B > 8$. Later, upon further exposure in the intercalate atmosphere, the A/B ratio becomes 'reversed' (maximum peak height, A, occurs at higher magnetic fields than the peak B), and its magnitude decreases down to value less than 2;55; the A/B maximum corresponds to the moment when the 'reversal' of CESR lineshape takes place (Fig. 2). The g_i (i=a, c) value of graphite CESR signal does not change up to its disappearance.

For the CESR signal with g_i* both the intensity, $I^*=(A^*+B^*)\times\Delta H^{*2}$, and linewidth, ΔH*, dependences vs. exposure time take a well-marked step-wise form (Fig. 3). At the moment of first observation the A^*/B^* value of this signal ~1, then the value of asymmetry parameter increases up to 3.8, forms a distinct peak and decreases up to 2.2 to the end of reaction (Fig. 6). The g_i*-values of this signal remain constant up to the end of intercalation.

DISCUSSION

With the configuration of our ESR experiment (Fig. 1) the microwave field penetrates into the HOPG plate mainly through its lateral sides, which are parallel to both the $\boldsymbol{c}$-axis and $\boldsymbol{H}_{rf}$ [11], i.e. through the lateral sides $h\times d$. Therefore, the evolution of graphite CESR signal of the sample investigated (Fig. 2) is mainly due to variations of the composition and properties of the HOPG plate at the surface areas from these sides. The dependence of the shape and intensity of graphite CESR signal on exposure time, τ, of a sample in HNO_3 vapours is qualitatively identical to that of the ESR signal lineshape and intensity of the localized spins in a metallic substrate on the thickness of a spray-coated film of another metal [12]. In our case, the spins in consideration are certainly mobile, but for $l/\delta_c<2$ the CESR line shape does not depend on spin mobility [11, 13, 14], i.e., in the framework of the Dyson theory [10] in HOPG plate investigated the spin carriers may be considered as localized. Therefore, the variations of the shape and intensity of the graphite CESR signal (Fig. 2 and 4) may be considered as being due to the formation of a macroscopic 'intercalation' layer on the HOPG plate (with conductivity being different from that of the initial material) and by advance of the interface separating this layer from as-yet the non-intercalated parts of sample (due to the diffusion of nitric acid molecules into the substrate along the graphite galleries). The invariability of the g-factor values for CESR signal from HOPG substrate (g_i) and that from 'intercalation' layer (g_i*) up to the disappearance of signal and the end of reaction, respectively, indicates that the interface between 'intercalation' layer and as-yet the non-intercalated parts of sample may be considered as non-conductive. The non-conductivity of this interface may be caused by significant distortion of a carbon net near the intercalation front and/or by the presence of high phase-boundary electrostatic potential due to the different current carriers concentration in the intercalated parts of graphite and in the non-intercalated ones.

In the experiments under consideration, the whole volume of sample investigated is available for CESR studies. Therefore, the time of the graphite CESR signal disappearance corresponds approximately to the moment of contact of the counter (antiparallel) intercalation fronts. Let us assume, that the intercalation is determined by a two-dimensional diffusion-controlled process, i.e. the thickness of the intercalated layer, d*, depends on the intercalation time, $\Delta\tau$, as $(d^*)^2=2D_{int}\times\Delta\tau$, where D_{int} is intercalate two-dimensional diffusion constant. In such a case, having substituted the value of time interval from the beginning of the graphite CESR signal transformation up to its disappearance (Fig. 2) and $d^*=l/2$ to this expression, it is easy to estimate the value $D_{int}\sim 2\times10^{-12}$ m^2 s^{-1}. It is worth to note that this value of D_{int} well correlates with that obtained by high-resolution neutron scattering by Simon et al. [15]: $D_{int}\cong 4\times10^{-12}$ m^2 s^{-1}.

A new and unexpected result of this experiment is the significant broadening of the graphite CESR signal from the beginning of the intercalation up to the contact of the counter intercalation fronts (Figs. 2 and 4). We suppose that the reason for it is the collisions of current carriers (at their diffusion along the graphite layers) with the non-conductive interface between the intercalated and the non-intercalated parts of the HOPG plate. Indeed, when the

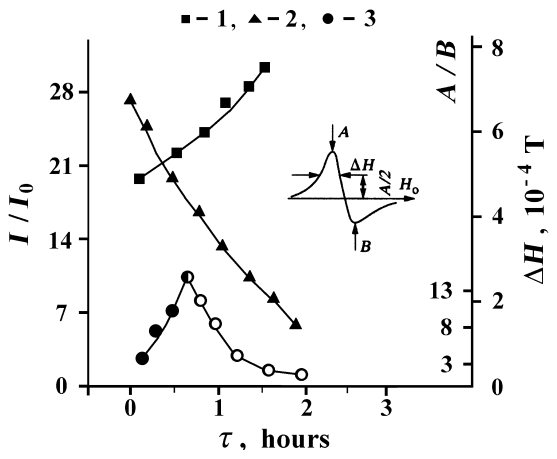

Figure 2. CESR lineshape parameters for non-intercalated parts of the narrow (l~$2\delta_c$) HOPG plate vs. exposure time, τ, in HNO_3 atmosphere. 1, 2 and 3 correspond to ΔH, A/B and I/I_0, respectively ($I=(A+B)\times\Delta H^2$; I_0 is the intensity of the Mn^{2+} ESR signal of the standard sample: $ZnS:Mn^{2+}$). The shaded and open dots are referred to the 'normal' and 'reversed' lineshape, respectively; half-shaded dot corresponds to the lineshape with symmetric phase with respect to the A peak. The X-band; T=300 K.

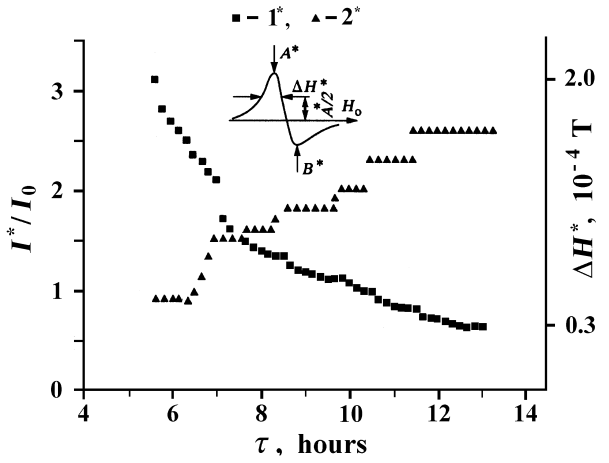

Figure 3. CESR lineshape parameters for intercalated parts of the narrow (l~$2\delta_c$) HOPG plate vs. exposure time, τ, in HNO_3 atmosphere. 1*, 2* and 3* correspond to ΔH*, A*/B* and I*/I_0, respectively (I* = (A*+B*)×ΔH*^{2}; I_0 is the intensity of the Mn^{2+} ESR signal of the standard sample: $ZnS:Mn^{2+}$. The X-band; T=300 K.

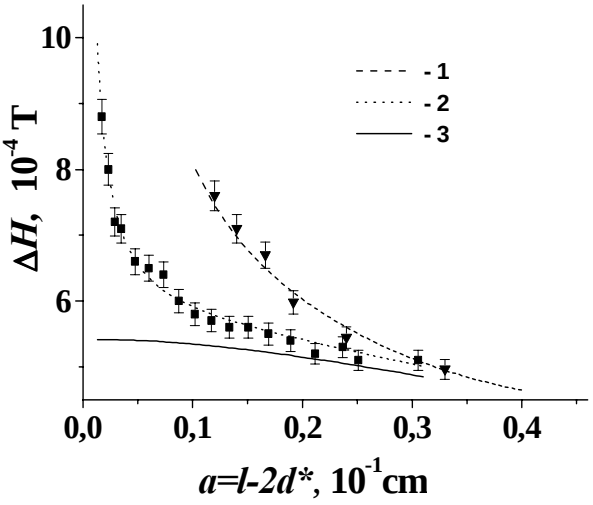

Figure 4. The experimental (dots) and theoretical (lines) values of CESR linewidth, ΔH, vs. thickness, a, of the non-intercalated (by HNO_3) part of HOPG plate (for two different samples). 1: G_a=30 cm^{-1}, T_2=1.15×10^{-8} s, δ_c=0.013 cm; 2: G_a=2 cm^{-1}, T_2=1.3×10^{-8} s, δ_c=0.02 cm; 3: G_a=0, T_2=1×10^{-8} s, δ_c=0.02 cm. $\boldsymbol{H}_0\|\boldsymbol{c}$, T=300 K.

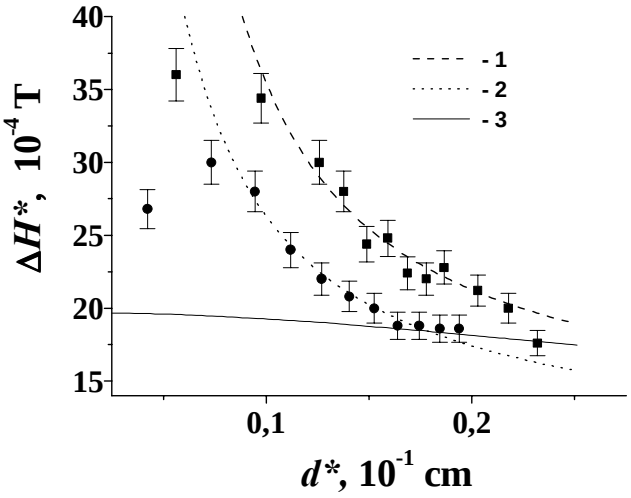

Figure 5. The experimental (dots) and theoretical (lines) values of CESR linewidth, ΔH*, vs. thickness, d*, of the intercalated (by HNO_3) part of HOPG plate (for two different samples). 1: G^*_a=180 cm^{-1}, T^*_2=0.38×10^{-8} s, δ_c=0.02 cm; 2: G^*_a=70 cm^{-1}, T^*_2= 0.45×10^{-8} s, δ_c=0.025 cm; 3: G_a=0, T_2=0.35×10^{-8} s, δ_c=0,025 cm. $\boldsymbol{H}_0\|\boldsymbol{c}$, T=300 K.

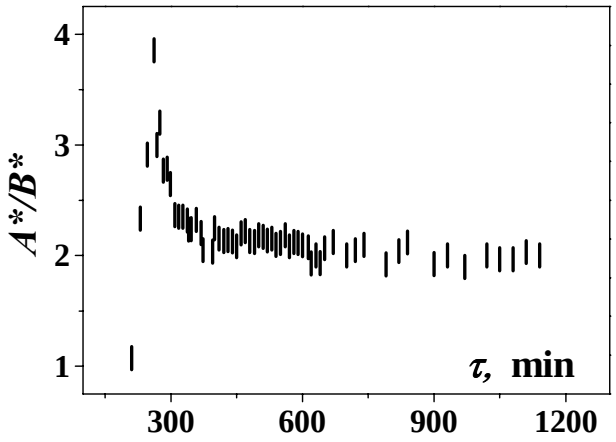

Figure 6. The CESR lineshape asymmetry parameter, A^*/B^*, of the intercalated part of HOPG plate vs. exposure time, τ, in HNO_3 atmosphere. The X-band; T=300 K.

intercalation front advances into the plate (due to the diffusion of nitric acid molecules into the graphite along the graphite galleries) the width of its non- intercalated part decreases and, therefore, the frequency of collisions of graphite current carriers with these interfaces increases. Therefore, assuming the probability of spin reorientation of graphite current carriers during such collisions to be non-zero, the increase of the total rate of spin relaxation of graphite current carriers (the graphite CESR linewidth) with the time of intercalation can be observed. Note, that in all previous ESR experiments on graphite intercalation [4-9] which were carried out on HOPG plates with $l>>\delta_c$, no such broadening of the graphite CESR signal was observed. This indirectly supports our interpretation of the graphite CESR signal broadening at the intercalation of the narrow ($l\sim2\delta_c$) HOPG plate.

The increase of $A^*/B^*(\tau)$ dependence at the beginning of intercalation from 1 until 3.7 (Fig. 6) corresponds to a theoretical $A/B(\lambda)$-dependence changing when increasing λ (λ is the ratio of a sample thickness to the skin-depth) [11, 13, 14]. At the constant value of electrical conductivity along the ***c***-axis of the forming GIC stage, this fact also points to the presence of the non-conductive barrier through the intercalation front and on its advance into sample. Under such understanding of the nature of $A^*/B^*(\lambda)$-dependence (Fig. 6) a changing of the skin-depth governed by the ***c***-axis conductivity of GICs from the beginning to the end of reaction may be easily determined by using the maximum and minimum values of A^*/B^* and the well known $A/B(\lambda)$-nomograms for different R-values [11, 13, 14]. Such kinds of calculations show that the skin-depths of the initial 7-th stage and of the final 2-d stage of GICs differ approximately in 1.6 times.

Using the relation $(d^*)^2=2D_{int}\times\tau$ the experimental dependence $\Delta H(\tau)$ can be easily transformed into the dependence $\Delta H(a)$, where $a = l-2d^*$ is the thickness of the non-intercalated part of HOPG plate (Fig. 4). The latter dependence can be calculated theoretically as well, using the exdended Dyson expressions for the CESR in metals including the effects of surface spin relaxation [10]. It is assumed in this theory that an electron colliding with the surface has a certain probability ε of spin reorientation, in addition to the steady probability $1/T_2$ (T_2 is the spin-relaxation time due to the collisions of current carriers with the imperfections in the sample volume) which exists for all electrons. In the general Dyson expressions for CESR line shape [10] the contribution of the surface spin relaxation effects to the CESR line shape is determined by the value of the term $Q=1/2G\times\theta$, where $G=3\varepsilon/4\Lambda$ (Λ is the mean free path of current carriers) and θ is the sample thickness. (The analysis of the mentioned Dyson expression has shown that at given sample thickness the CESR linewidth increases with G value. For $G\neq0$, the value of CESR linewidth tends to the infinity at $\theta\rightarrow0$). Obviously, if $\varepsilon \equiv \varepsilon_a$ is considered as an average value of probability of spin reorientation during collisions of graphite current carriers with the non-conductive phase boundary, then the extended Dyson expressions for the CESR in metals including the effects of surface spin relaxation of current carriers can be used for analysis of $\Delta H(a)$ dependence also. It is shown in Fig. 4, where the results of such analysis are presented, that the theoretical dependence of the graphite CESR linewidth, with non-zero values of $G=G_a$ describes the experimental data well. The found value of G_a=1 (10) cm^{-1} and the typical HOPG values of $\Lambda\equiv\Lambda_a=(0.4\div1.6)\times10^{-5}$ cm [16] correspond to $\varepsilon_a=(0.5\div2.1)\times10^{-4}$ ($(0.5\div2.1)\times10^{-3}$). It is worth noticing that at present there are no data on interface spin relaxation in conductors in literature. There are only some published data on surface spin relaxation in simple metals. For comparison, the surface spin reorientation probabilities of conduction electrons in Cu and Li bulk samples are equal to $\sim10^{-2}$ [17] and $\sim5\times10^{-6}$ [18], respectively.

It is obvious, that the spins of current carriers colliding with the front of reaction from the intercalated part of graphite also have some probability of reorientation, ε_a^*, during such collisions. Therefore, the analysis of $\Delta H^*(\tau)$-dependence (Fig. 5) it is possible to execute on the same procedure, which above was used for the analysis of the $\Delta H(\tau)$-dependence (Fig. 4). The application of the specified technique of the analysis to the experimental $\Delta H^*(\tau)$-dependences (Fig. 5) give the G_a^*-values: ~180 cm^{-1} in one experiment and ~70 cm^{-1} in the other experiment. As we see, both values of G_a^* appreciably greater than the values of G_a. If $\varepsilon_a=\varepsilon_a^*$, it means that

already in the GIC stage originally forming the mean free path of current carriers in a basal plane appreciably shooter, than in initial graphite.

Conclusions

In this work the results of an *in situ* conduction ESR (CESR) study of HNO_3 molecule intercalation into narrow highly oriented pyrolytic graphite (HOPG) slabs are presented. The changes in the graphite CESR signal line shape, intensity and linewidth and the stepwise changes both of intensity and linewidth of CESR signal from intercalated sample have been clearly detected during this reaction. Under the assumption that the graphite CESR signal evolution is caused by the advance of a boundary separating the intercalated and non-intercalated HOPG, the average value of spin reorientation probability during the collision of current carriers with this interface and the constant of two-dimensional diffusion of nitric acid molecules into HOPG have been extracted from experimental data. Basing on the results obtained it may be supposed that many of existing problems connected with application of CESR technique to the study of graphite and other conducting carbon materials intercalation will be successfully solved after introducing into consideration interface spin relaxation effects. Now the works in this direction are in progress.

References

1. Dresselhaus MS, Dresselhaus G. Intercalation compounds of graphite. Adv. Phys. 1981; 30(2):139-326.
2. Solin SA, Zabel H. The physics of ternary graphite intercalation compounds. Adv. Phys. 1988; 37(2):87-254.
3. Lagrange P, Herold A, Herold C. Why mono- or polylayered intercalated sheets in graphite-electron donors systems? Mol. Cryst. Liq. Cryst. 1998; 310:33-42.
4. Davidov R, Milo O, Palchan I, Selig H. ESR study of graphite-fluorine and graphite-fluoride acceptor intercalation compounds. Synth. Met. 1983; 8:83-87.
5. Palchan I, Davidov D, Zevin V, Polatsek G, Selig H. An in situ ESR study of the intercalation mechanisms: HOPG/fluorine and HOPG/HNO_3. Synth. Met. 1985; 12:413-418.
6. Palchan I, Mustachi F, Davidov D, Selig H. ESR study of dulate intercalation compounds: C/F, C/K/F and C/Li/F. Synth. Met. 1984/85; 10:101-106.
7. Nakajima M, Kawamura K, Tsuzuku T. ESR study of HNO_3 intercalation process of graphite. J. Phys. Soc. Jpn. 1988; 57(5):1572-1575.
8. Ziatdinov AM, Tsvetnikov AK, Mishchenko NM, Sereda VV. In situ ESR studies of intercalation of SbF_5 molecules into highly oriented pyrolitic graphite. Mat. Sci. Forum (Intercalation Compounds - ISIC-6) 1992; 91-93:583-588.
9. Ziatdinov AM, Mishchenko NM. In situ ESR study of the HNO_3-intercalate diffusion process in graphite intercalation compounds. J. Phys. Chem. Solids 1997; 58(7):1167-1172.
10. Dyson FJ. Electron spin resonance absorption in metals. II. Theory of electron diffusion and the skin effect. Phys. Rev. 1955; 98(2):349-359.
11. Ziatdinov AM, Mishchenko NM. Electron spin resonance lineshape and kinetic parameters of the conduction electrons in highly anisotropic conductors: highly oriented pyrolitic graphite. Phys. Solid State 1994; 36(8):1283-1289.
12. Zevin V, Suss JT. ESR in layer-substrate structures: The line shape and nondestructive contactless measurements of the layer conductivity. Phys. Rev. 1986; B34(10):7260-7270.
13. Saint Jean M, McRae EP. Planar diffusion constant D_a in acceptor-graphite intercalation compounds. Phys. Rev. 1991; B43: 3969-3974.
14. Kodera HJ. Dyson effect in the electron spin resonance of phosphorus doped silicon. Phys. Soc. Jpn. 1970; 28(1):89-98.
15. Simon C, Rosenman I, Batallan F, Rogerie J, Legrand JF, Magerl A, Lartigue C, Fuzellier H. Measurement of defect mobility in a defect-mediated melting. Phys. Rev. 1990; B41(4):2390-2397.
16. Spain IL. Electronic transport properties of graphite, carbons, and related materials. Walker PL, Throweer Jr and PA, editors. Chemistry and physics of carbon, vol 8, New York:Dekker, 1973:119-305.
17. Walker MB. Surface relaxation and quasiparticle interactions in conduction-electron spin resonance. Phys. Rev. 1971; B3(1):30-41.
18. Zhikharev VA, Kessel AR, Kharakhashian EG, Cherkasov FG, Svarts KK. Conduction Electrons spin echo in metals. Soviet Phys.- JETP 1973; 64(4):1356-1366.

Acknowledgments

The author is grateful to N.M. Mishchenko, V.V. Kainara for help in experiments and calculations and to L.B. Nepomnyashchii (Scientific Research Centre for Graphite, Moscow) for providing the HOPG samples.

This work was partially supported by the Russian Foundation for Basic Research (grant No. 00-03-32610).